Kovove Mater. 59 2021 245–256
DOI: 10.4149/km_2021_4_245

Investigation of mechanical and microstructural properties of AA5754/AA6013 dissimilar aluminium alloys joined by GMAW and FSW methods

A. Yürük[1], Y.Ayan[2], B. Çevik[3]*, N. Kahraman[2]

[1]*Borsa Istanbul Vocational and Technical Anatolian High School, Düzce, Turkey*
[2]*Department of Manufacturing Engineering, Karabük University, Karabük, Turkey*
[3]*Department of Machinery & Metal Technologies, Düzce University, Düzce, Turkey*

Received 22 April 2021, received in revised form 7 July 2021, accepted 7 July 2021

Abstract

Aluminium alloys AA5XXX and AA6XXX have low density and high yield strength and are frequently used to make air, sea, and land vehicles/technology lighter. Different types of aluminium alloys need to be adaptively assembled together. Therefore, it is important but difficult to weld aluminium alloys. This study investigated the microstructural and mechanical properties of two dissimilar aluminium alloys, AA5754 and AA6013, which were welded using gas metal arc welding (GMAW) and friction stir welding (FSW). Hardness, tensile, bending, and fatigue tests were done on the welded samples. The test results were evaluated and interpreted according to the literature. The weld zone (weld metal, HAZ) of AA5754 and AA6013 aluminium alloys joined by GMAW and FSW showed significant differences. The highest tensile strength and fatigue life were obtained from the FSWed sample after the base metals. The welded samples joined using both welding methods were successfully deformed by 180° without damaging their upper or lower surfaces.

K e y w o r d s: FSW, GMAW, AA5754, AA6013, microstructure, fatigue strength

1. Introduction

One key issue in producing new generation technology is to do studies on lowering energy consumption by considering environmental impact. Many sectors are constantly researching ways to minimise CO_2 emissions and reduce costs by reducing weight [1–4]. In studies that focus on reducing energy consumption, it is common for engineers to prefer to use lightweight metals/materials. Such studies thus tend to highlight light metals [4–6]. For designers and engineers, aluminium and its alloys are some of the most promising light metals. They are widely used to reduce weight [2–4, 6, 7]. Moreover, they offer many application areas in the aerospace, automotive, and marine industries because they are light, highly resistant to corrosion, and non-flammable – unlike polymer matrix composites [5–8].

5xxx series aluminium alloys are made from aluminium and magnesium (Al-Mg) alloys [9]. 5754 series aluminium alloys are widely used in the manufacturing of marine vehicles because they are light and have superior corrosion resistance in an atmospheric environment. They also are used in architecture, pressure vessel and fuel tank manufacturing, and welded chemical and nuclear buildings [7, 9]. 6xxx series aluminium alloys are made from aluminium-magnesium-silicon-(copper) (Al-Mg-Si-(Cu)) alloys [10]. 6013 series Al alloys are widely used in aircraft manufacturing (i.e., the aerospace industry) because they are light and have high strength [10, 11]. The need arose to weld this aluminium and its alloys used in such a wide area [7, 10, 12]. However, welding aluminium and its alloys is difficult due to reasons such as high heat conduction, the presence of the Al_2O_3 layer on the surface, and the absence of annealing colour during melting [7, 12, 13]. Many solutions for welding certain aluminium alloys have emerged in the past twenty years. Nevertheless, common issues such as porosity, excessive material loss, and hot crack when welding certain alu-

*Corresponding author: e-mail address: bekircevik@duzce.edu.tr

minium alloys have yet to be solved [10–17].

Friction stir welding (FSW) is a solid-state welding method. It can be used to weld metals and polymers [10, 11]. FSW is performed by first immersing a stirring tool rotating at high speed into two face-to-face fixed plates and then advancing that at a certain speed. The stirring tool used in the welding process contains two parts: a pin and a shoulder [16, 18, 19]. Friction heat occurs at the contact point when the shoulder part of the stirring tool meets the materials and rotates at high speed. The yield strength of the materials decreases and plastic change occurs under the impact of heat. The pin stirs the material, resulting in joining [10, 19, 20]. The aerospace, shipbuilding, rail vehicle system, and automotive industries frequently use this method to weld aluminium, copper, and titanium alongside their respective alloys, as well as certain types of steel [16–21].

Gas metal arc welding (GMAW) is an ideal fusion welding method for the mass production of applications where both steels and nonferrous metals such as aluminium and titanium are used. In GMAW, the heat required for welding is generated through the arch that forms between the piece of metal and welding wire – which continuously gets transferred to the weld zone and melts. During welding, the welding wire is sent to the arc area automatically; it melts and forms the weld metal [22–24]. The weld zone is shielded by a shielding gas (active or inert). When welding aluminium alloys using GMAW, argon (Ar), helium (He), or Ar-He mixtures at different ratios can be used as a shielding gas [23, 24]. GMAW can be integrated into robotic systems – where all parameters can be kept under control. It, in turn, lowers the chance of defects emerging due to the operator and the properties of the material [24–26].

Welding is important manufacturing technology. It maintains its popularity because it joins steels and nonferrous metals and yields high-quality joints [14–16]. However, the increase in the variety of materials used in the industry requires the welding of dissimilar metals. Furthermore, the increasing importance of economic factors, especially in recent years, makes welding of dissimilar materials to one another necessary [7, 10, 13, 14, 16]. However, different mechanical, metallurgical, and chemical properties make welding difficult for dissimilar metals and alloys [13, 15, 26]. Therefore, welding dissimilar aluminium and alloys attracts the attention of engineers, and researchers, in turn, intensively continue to research the topic. Lean et al. [27] welded AA6082 and AA6092/SiC/25p composite materials using MIG, and then they investigated the mechanical and microstructural properties of the welded joints. They found that porosities forming in the weld seams had a negative effect on their mechanical properties. Caglioni et al. [28] welded different combinations of aluminium alloys (5383/5383, 5754/5754, 6005/6005, 5754/5383, and 6005/5383, and 6005/5754) using MIG welding and then examined their mechanical and microstructural properties. They discovered that the yield and tensile strength of similar aluminium alloys were higher than those of dissimilar aluminium alloys. Cole et al. [29] welded AA6061 and AA7075 aluminium alloys using FSW and then investigated the effect of the position of aluminium alloys and the tool plunge depth on the welded joints. They reported higher mechanical properties when they placed softer material on the advanced side during welding. Khanna et al. [30] welded AA6061-T6 and AA8011-H14 aluminium alloys using FSW and then studied their mechanical and microstructural properties. They found that the position of dissimilar aluminium alloys during welding affected the mechanical properties and microstructure of the welded joints. The literature indicates that the problems encountered during the welding of dissimilar aluminium alloys by GMAW and FSW could not be solved completely. Therefore, further studies are needed to examine the welding of aluminium alloys [22–26].

In this study, the researchers welded AA5754/AA6013 aluminium alloys using GMAW and FSW. They then examined their macrostructural and microstructural properties at the weld zone of the samples and carried out hardness, tensile, bending, and fatigue tests on them. The test results were assessed and interpreted based on the literature.

2. Experimental

2.1. Materials

In this study, AA5754/AA6013 aluminium alloys cut into $5 \times 100 \times 500\,\mathrm{mm}^3$ were used. H111 was used to manufacture AA5754 aluminium alloy, and T6 heat treatment was used to manufacture AA6013 aluminium alloy. Table 1 shows the alloys' chemical compositions. Table 2 shows their mechanical properties.

2.2. MIG welding process

AA5754 and AA6013 were welded face-to-face using automatic GMAW. Before the welding, the samples were fixed face-to-face without any void. The welding took place using 1.2 mm diameter additional wire (AWS A510: ER5356). Table 3 shows the chemical composition of the welding wire. Table 4 shows the wire's mechanical properties. Welding was conducted unilaterally using an automatic Fronius TransSynergic 4000 Comfort synergic welding machine; the researchers chose a welding speed of $150\,\mathrm{mm\,min}^{-1}$ and a welding current of 150 A. After welding, the samples were left to cool to room temperature.

Table 1. Chemical compositions of AA5754 and AA6013 aluminium alloys (wt.%)

	Si	Fe	Cu	Mn	Mg	Cr	Zn	Ti	Al
AA5754	0.40	0.4	0.10	0.5	2.6–3.6	0.3	0.20	0.15	Rest
AA6013	0.7	0.3	0.9	0.3	0.9	0.03	0.07	0.02	Rest

Table 2. Mechanical properties of AA5754 and AA6013 aluminium alloys

	Tensile strength (MPa)	Elongation (%)	Hardness HB
AA5754	242.4	16.2	50–55
AA6013	369.4	15.5	130

Table 3. Chemical properties of the welding wire (wt.%)

Si	Fe	Cu	Mn	Mg	Cr	Zn	Ti	Al
0.25	0.4	0.1	0.05–0.2	4.5–5.5	0.05–0.2	0.1	0.06–0.15	Rest

Table 4. Mechanical properties of the welding wire

Tensile strength (MPa)	Elongation (%)
240–296	17–27

2.3. FSW process

A stirring tool with an adjustable pin length was designed and built specifically to carry out FSW. It contains two parts: a shoulder and a pin. The shoulder was made of X210Cr12 (a cold work tool), and the pin was made by machining an M6 × 1 HSS guide tool at a 3° angle. The hardness of the shoulder was raised to 50 HR_C using heat treatment. The pin's height was adjusted to 4.8 mm. Welding was carried out using an Arsenal FU251M milling machine. Before welding, AA5754/AA6013 aluminium alloys were fixed face-to-face. The tool's shoulder was then immersed at a constant shoulder plunge depth of 0.2 mm. The welding took place at a speed of 25 mm min^{-1}, at 1250 rpm. Figure 1 shows the schematic view and the welding process plan of the stirring tool.

First, a macro examination was carried out on the welded samples joined by automatic GMAW and FSW. The samples with an ideal upper surface and lower surface properties and weld penetrations were selected as 'optimum'. Then, mechanical and metallurgical/metallographic properties of the samples welded at the optimum welding parameters were examined.

2.4. Test operations

First, macrostructure and microstructure examinations, followed by hardness, tensile, bending, and fatigue tests were carried out on the samples joined using GMAW and FSW. The test samples were cut with a water jet. The samples taken from the perpendicular section to the welding direction were then sandpapered using 600, 800, 1000, and 1200 no. sandpapers, and finally polished using a 1 µm of polishing felt and 3 µm of diamond paste. The samples were etched for approximately 90 s using Keller's reagent (150 ml H_2O, 3 ml HNO_3, 6 ml HF). Microstructure examinations were carried out on a Metkon inverted metal microscope. Micro images were taken from the transition zones of the weld and at the weld centre. Hardness

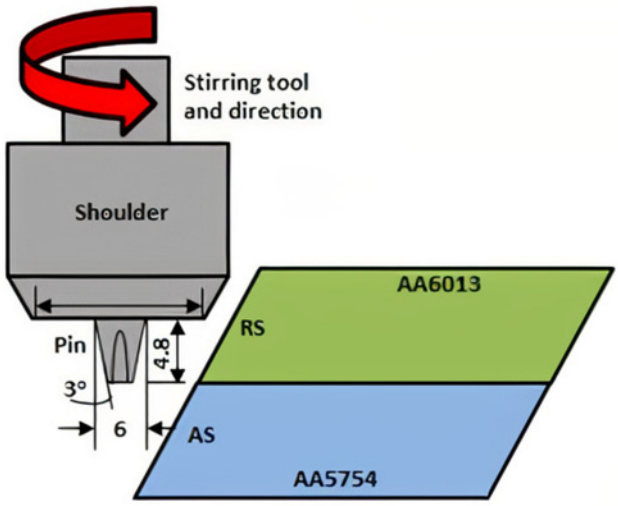

Fig. 1. Positioning of the stirring tool and aluminium parts.

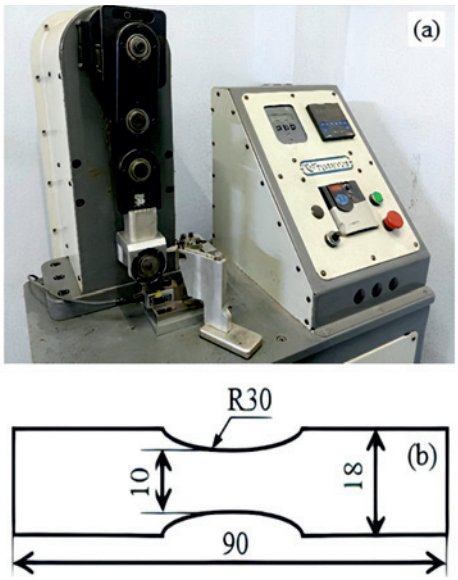

Fig. 2. (a) Fatigue test device and (b) fatigue test sample.

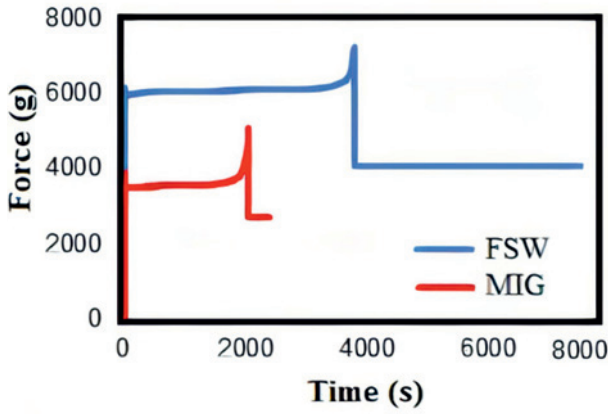

Fig. 3. Force-time graphs of the welded samples.

tests were carried horizontally on samples taken from the perpendicular section to the welding direction. During each of the experiments, hardness measurements were taken using DUROLINE M Micro-Vickers hardness tester by applying 100 g load for 10 seconds. Then, hardness was measured over 29 points at 1 mm intervals, starting from the weld centre. The tensile, bending, and fatigue test samples were prepared in accordance with TS EN ISO 4136, EN ISO 5173, and ASTM E466-07 standards, respectively. Both tensile and bending tests were carried out at room temperature using a Shimadzu tensile device (with a capacity of 50 kN). The tensile tests were carried out at $0.5\,\mathrm{mm\,min^{-1}}$, while the bending tests were carried out at $5\,\mathrm{mm\,min^{-1}}$. The fatigue tests were carried out using a computer-controlled bending fatigue test device designed and produced for this study. Figure 2 shows the dimensions of the fatigue test device and fatigue test sample.

Fatigue tests were carried out at six amplitude values on each welded sample (all joined at different welding parameters), at a frequency of 10 Hz, and at room temperature. For each amplitude value, two samples were tested; the average values of data collected from both were then used to calculate fatigue strength. Figure 3 shows load-time graphs from the fatigue test for all welded samples joined by GMAW and FSW. Using load-time graphs, the researchers calculated the bending and shear stresses of the samples. The fatigue strength of the welded joints was found by calculating the combined proof stress of both stresses. The load cell of the fatigue test device gives the load in grams. Hence, when calculating the fatigue strength, the researcher carried out the operations by converting the load into force (Newton). First, the moment caused by the bending force was calculated using Eq. (1) to calculate the bending stress caused by the force applied during fatigue tests. Then, the values required to calculate the fatigue stress were found by calculating the polar moment of inertia in Eq. (2). Bending stress was calculated in Eq. (3) – with the help of the data from the calculations for the bending moment and moment of inertia. Additionally, the shear stress caused by the force in the weld was calculated with the help of Eq. (4); however, the researchers did not consider it during calculations since its effect on fatigue stress was negligible. Finally, the fatigue stress was calculated using Eq. (5).

$$M_{\mathrm{bending}} = F \times L, \tag{1}$$

$$W = \left(b \times h^2\right)/6, \tag{2}$$

$$\sigma_{\mathrm{bending}} = M_{\mathrm{bending}}/W, \tag{3}$$

$$M_{\mathrm{bending}} = F \times L, \tag{4}$$

$$\sigma_{\mathrm{R}} = \sqrt{\sigma_{\mathrm{bending}}^2 + 3\tau^2}, \tag{5}$$

where M_{bending} is bending moment (N mm), F is the applied force (N), L is the length (mm), W refers to the moment of inertia ($\mathrm{mm^4}$), b is the width (mm), h is the height (mm), A is the area ($\mathrm{mm^2}$), $\sigma_{\mathrm{bending}}$ is the bending stress (MPa), τ is the shear stress (MPa), and σ_{R} refers to the fatigue stress (MPa). Wöhler's (S-N) fatigue graphs were drawn up by using the fatigue stresses from the calculations and the number of cycles obtained during the tests as a point of reference. The fracture surface of each sample was analysed on a Carl Zeiss Ultra Plus Gemini Fesem scanning electron microscope (SEM).

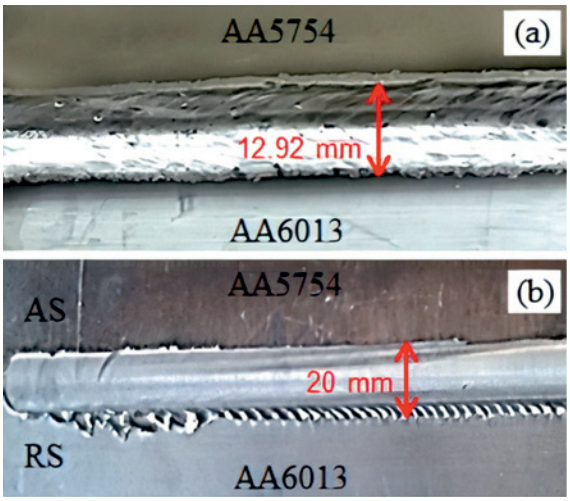

Fig. 4. Macro images of the welded samples: (a) GMAW and (b) FSW.

3. Results and discussion

3.1. Macrostructure

Figure 4 shows weld zone macro images of the welded samples of AA5754/AA6013 aluminium alloys that were welded using GMAW and FSW. The macro image of the weld seam joined by GMAW revealed no macro weld defects (joint defects, transverse and longitudinal cracks, undercut defects, crater cracks, splashing) that would negatively affect the mechanical properties of the welded joint. In addition, there was no significant angular distortion in the transverse or longitudinal direction of the welded plate (GMAW). Eliminating the operator factor by means of choosing the welding parameters (e.g., welding current, welding voltage, welding speed) within a correct range and performing welding operations in an automatic welding machine in the welding process played an important role in these GMAW results. Çevik and Koç [24] reported that using an automatic welding machine – in which all welding parameters can be controlled during the MIG welding of 5754 aluminium alloy – kept both width of the weld seam and the amount of accumulated metal constant throughout the weld seam. It also generated nice-looking weld seams. A joining defect occurred as long as the stirring tool diameter at the start and end points of the FSWed AA5754/AA6013 aluminium alloy sample. The upper surface image of the FSWed plate revealed no macro-scale surface defects in the weld seam.

On the other hand, corrugation and burrs formed on the retreating side (RS) of the weld seams of the plates. This occurred because the stirring tool scraped the material on the friction surface towards the direction of the rotation (AA6013 side), whereas the shoulder part rotated during the friction of the stirring tool against the plate at high speed. This corrugation was also affected by the ductility and high deformability of AA5754 and AA6013 aluminium alloy plates. Corrugations did not form on the advanced side (AS). Uygur [31] reported that a stirring tool shoulder caused high heat input. The resultant softening of the materials during its friction to the welded plates and the stirring tool put the burrs towards the edge in the direction of the rotation.

3.2. Microstructure

Figure 5 shows weld zone microstructures of the AA5754/AA6013 aluminium alloy samples welded by GMAW and FSW. Images of their microstructures were taken from the weld centre and transition zones. Both welding wires melted, and the aluminium plates melted and solidified locally, thus forming the weld metal due to the arc between the plates welded face-to-face with welding wire during GMAW. High heat input applied locally during welding transformed the previous microstructural properties of the aluminium alloys both in and near the melting zone. Therefore, the microstructure of the weld metal formed in a different character than both base metals. The grains in the weld metal and HAZ became coarser. Yeni et al. [32] expressed that the heat input during MIG welding of aluminium alloys caused grain coarsening in the heat-affected zone (HAZ) and the weld metal. In addition, the weld metal grains in the transition zone appear to have formed by directing towards the weld centre. A microstructure review of the weld zone revealed no microstructural weld defects such as macro- and microporosity, microcracks, and hot cracks. However, the coarsening in HAZs was not the same on either side of the weld seam. The HAZ of AA6013 aluminium alloy had a more refined grain structure than the HAZ of AA5754 aluminium alloy. This was associated with the chemical composition and precipitate structure of AA6013 aluminium alloy [9, 10, 27].

The microstructure images of the FSWed sample revealed that the weld metal was separated from the base metals with clear boundaries. Weld metals expanding towards the upper surface of the plates had formed due to the high heat input caused by the friction of the stirring tool towards the upper part of the plates during FSW. This appears to have been caused by the upper part of the plates reaching maximum temperature, the lower part of the plates dropping to lower temperatures due to the friction caused by the stirring tip. A closer look at the microstructure of the transition zone of the welded joint revealed that micro-void defects formed in certain regions. A high amount of plastic deformation occurred due to high heat input and stirring at high speed, especially in the weld metal during FSW [11, 19, 22]. Therefore,

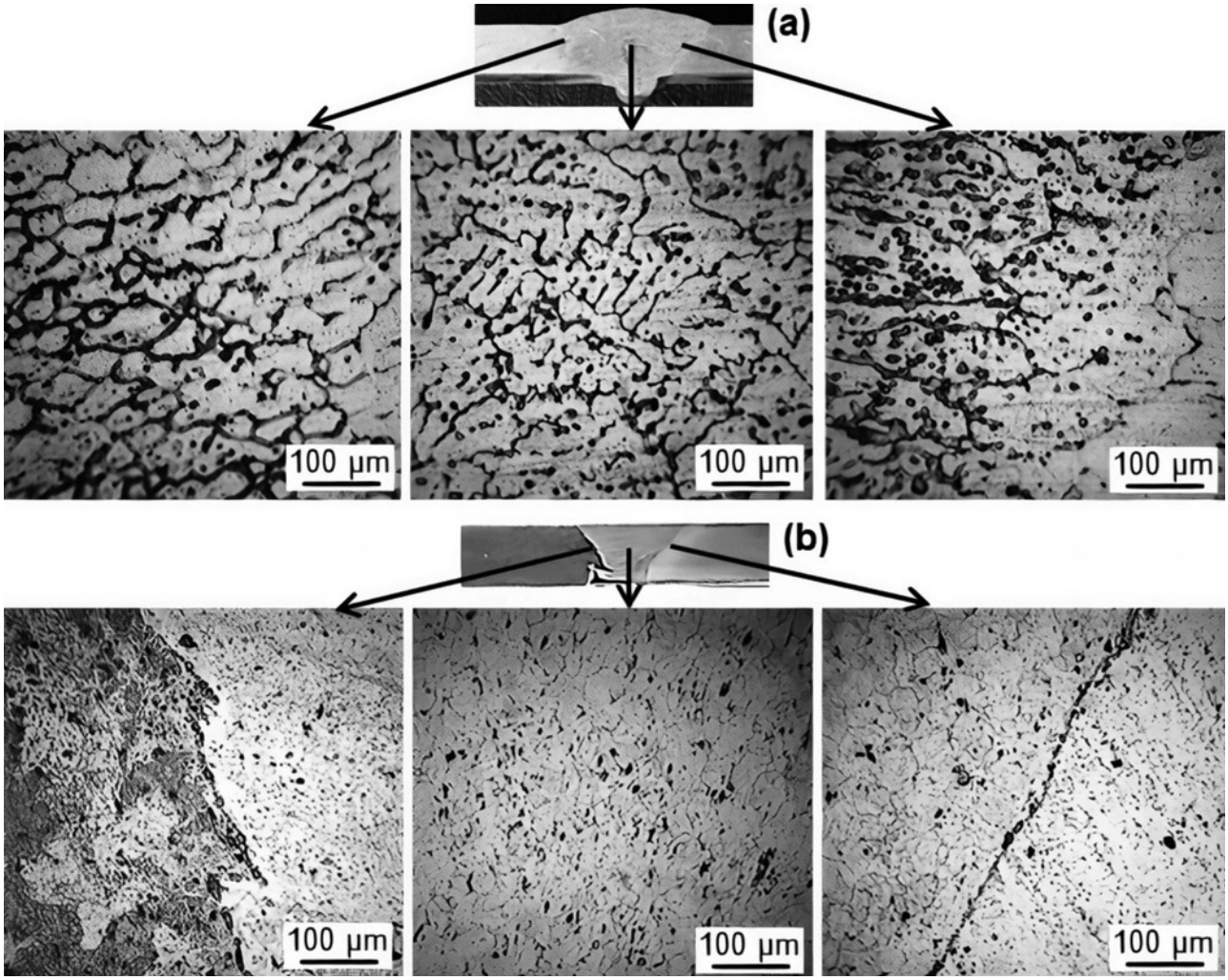

Fig. 5. Microstructures of the weld zone: (a) GMAW and (b) FSW.

the weld metal on all welded samples formed from a homogeneous mixture of both base metals due to high deformation. The microstructures of weld metal were made up of coaxial dynamically recrystallised grains. Çevik et al. [18] found that weld metal showed a coaxial microstructure due to the dynamic recrystallisation caused by heat and plastic deformation during FSW. The HAZs and weld metal images of AA5754/AA6013 aluminium alloys welded using different methods revealed that weld metals, HAZs, and zones close to the weld metal exhibited distinctly different images to each other in both joints. While the weld metal of the GMAW-welded sample was composed of coarse dendritic grains, the weld metal of the FSWed sample was composed of finer coaxial grains.

3.3. Hardness

Figure 6 shows the hardness distribution of the weld zone of the GMAW and FSW-welded AA5754/AA6013 aluminium alloy samples. The hardness graph reveals that HAZ hardness was lower than that of the base metals in each welded joint. In other words, the AA6013's HAZ was lower than the hardness of the AA6013 base material. Similarly, the AA5457's HAZ was lower than the hardness of the AA5457 base material. In both welded joints, the hard zone was measured in AA6013 aluminium alloy. The welding wire melted, the aluminium plates locally melted and solidified, and weld metal formed due to the arc forming between the AA5754/AA6013 aluminium alloy plates joined face-to-face with the welding wire during GMAW. Therefore, the weld metal had different hardness characteristics from both base metals [26–28]. The highest hardness value obtained at the weld centre of the sample welded by GMAW was 66.1 $HV_{0.1}$. Likewise, the lowest hardness value on the weld centre(s) was 64.5 $HV_{0.1}$ in the HAZ of AA6013 and 53.2 $HV_{0.1}$ in the HAZ of A5754. The highest hardness values were 100.5 $HV_{0.1}$ in the HAZ of AA6013, and 59.6 $HV_{0.1}$ in the HAZ of AA5754. The AA5754/AA6013 aluminium alloy plates which

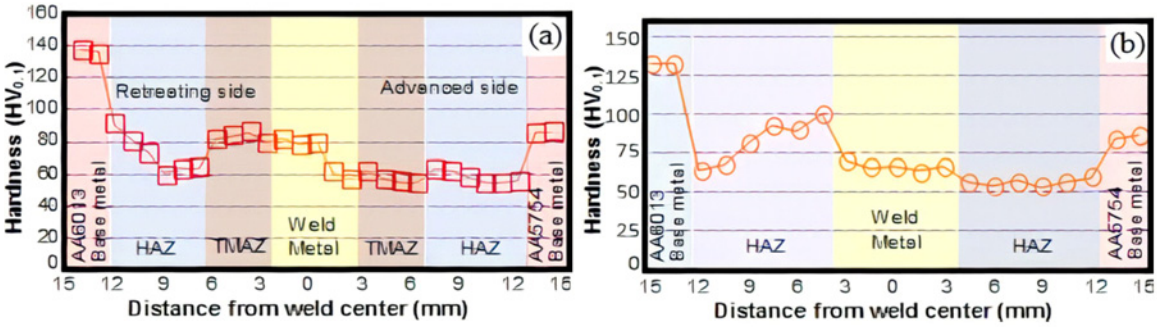

Fig. 6. Hardness distributions of weld zone: (a) FSW and (b) GMAW.

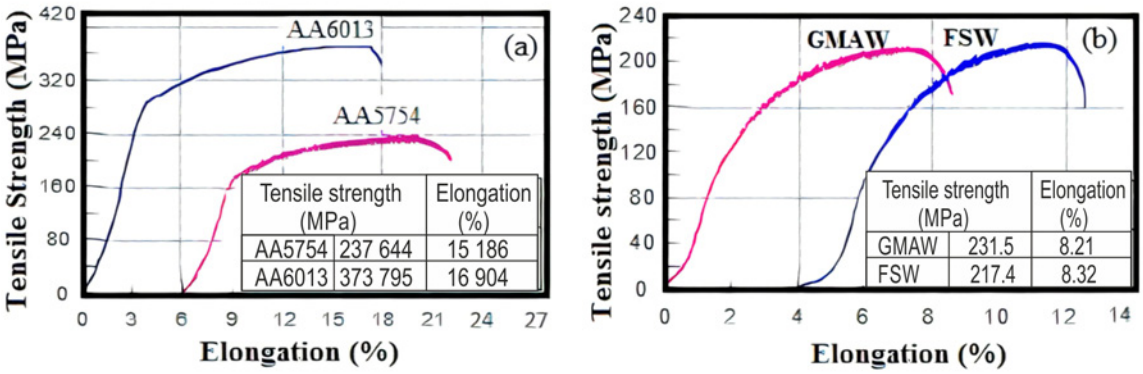

Fig. 7. Tensile test results: (a) base metals and (b) welded samples.

were placed face-to-face during FSW were exposed to high deformation. This was due to the stirring tool rotating at a high rpm and the weld metal formed with the mixture of both base metals because of stirring. Therefore, the hardness of the weld metal exhibited hardness characteristics that were different from both base metals. The highest hardness value at the weld centre of the FSWed sample was 79 $HV_{0.1}$. The lowest hardness values of the weld zone of the FSWed sample were 60.3 $HV_{0.1}$ in the HAZ of AA6013 and 60.2 $HV_{0.1}$ in the HAZ of AA5754. The highest hardness value in the HAZ of AA6013 was 91 $HV_{0.1}$, and the highest hardness value in the HAZ of AA5754 was 61.8 $HV_{0.1}$. Accordingly, the hardness values of the weld zones from both welding methods decreased compared to the base metals. However, comparing the AA6013 aluminium alloy side of the welded samples revealed higher results in the sample welded using GMAW. This might be caused by the fact that hardening precipitates in the HAZ of ageing heat-treated AA6013 aluminium alloy had dissolved. In addition, these precipitates re-gained a slight hardening property due to ageing caused by the effect of heat input [26].

3.4. Tensile strength

Figure 7 shows tensile test results of the GMAW and FSW-welded AA5754/AA6013 samples. Tensile test results revealed that the mean tensile strength and elongation % value of AA5754 Al alloy were 237.6 MPa and 15.18 %, respectively. The mean tensile strength and elongation % value of AA6013 Al alloy were 373.7 MPa and 16.94 %, respectively. The mechanical properties of AA603 aluminium alloy were higher compared to those of AA5754 aluminium alloy that was annealed and subjected to a slightly colder forming hardening process (H111) during stretching or levelling – due to the solution heat treatment and artificial ageing (T6 heat treatment) applied during the production of AA6013 aluminium alloy [26]. GMAW is a melting welding-based method. Therefore, both welding wire melted and the aluminium plates locally melted and solidified to form the weld metal due to the weld arc which formed between welding wire and the AA5754/AA6013 aluminium alloy plates during welding. In this case, the weld metal was made up of welding wire – a mixture of AA5754 and AA6013 aluminium alloy. The tensile strength and elongation of the welded sample joined by GMAW were 213.5 MPa

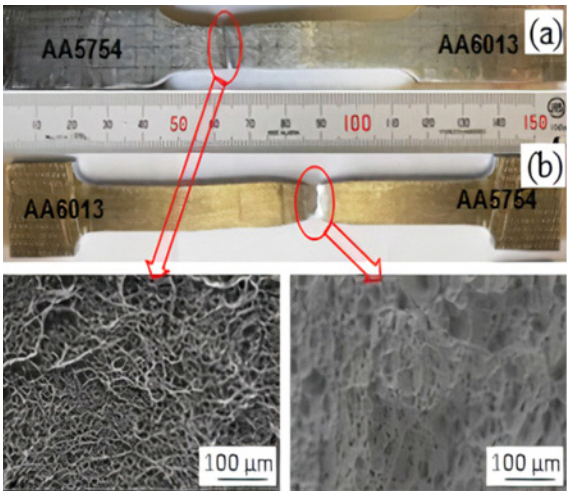

Fig. 8. Fracture behaviour of welded tensile test samples: (a) GMAW, (b) FSW.

and 8.21 %, respectively. Similarly, the tensile strength and elongation of the FSWed sample were 217.4 MPa and 8.32 %, respectively. High heat input, melting, and solidification during GMAW caused the properties of the welded alloys to deteriorate during their production partially. This caused the tensile strength and % elongation of the joint welded by GMAW to decrease compared to the base metals. When the tensile test results of the sample welded by GMAW were compared with AA5754 aluminium alloy, they found that tensile strength decreased by 10.15 %, and the elongations dropped by 45.91 %. When the tensile test results of the same sample were compared with AA6013 aluminium alloy, it was discovered that the tensile strength dropped by 42.88 %, and the elongation decreased by 51.53 %. The microstructural transformations, which took place during melting and solidification, caused lower tensile strength and elongation amount of the GMAW-welded joint compared to the base metals. The fracture of the GMAW-welded sample occurred in the HAZ of the AA5754 side with the lowest hardness (Fig. 8a). Çevik and Koç [24] reported that the heat input during MIG-welding of aluminium alloys decreased the properties acquired by the base metal during production, and this, in turn, had a negative effect on the mechanical properties of the welded joints.

During FSW, the weld zone was exposed to heat input and an intense deformation due to the stirring tool rotating at high speed. During this process, the metal in the weld zone softened. Micro grains in base metals also softened during this period, broke down due to intense deformation, and then turned into finer micro grains. In addition, the pin part of the stirring tool wanted to transfer the grains in the weld zone from the lower surface of the plates to their upper surface. This was due to the effect of rotation at a high rpm; however, the shoulder part compressed and concentrated the material in this zone – which was mixed and transferred upon the application of pressure. During these processes, micro porosities formed at the interface between the weld metal and the thermomechanically-affected zone (TMAZ). Therefore, the tensile and elongation amounts of the FSWed joints were lower compared to the base metals due to micro porosities that formed because of heat input and dense plastic deformation exposed by the weld zone during welding. Azimzadegan and Serajzadeh [33] reported that hardness decreased in HAZ due to the heat input forming in the weld zone of FSWed aluminium alloys, noting that these zones negatively affected the mechanical properties of welded joints. A comparison of the tensile test results of the FSWed sample with AA5754 aluminium alloy revealed a drop in tensile strength by 8.51 % and a drop in % elongation by 45.19 %. A comparison tensile test results of the same sample with AA6013 aluminium alloy revealed a 41.83 % drop in tensile strength and a 88 % drop in % elongation. In the FSWed sample, the fracture occurred from the zone between TMAZ-HAZ on the AA5754 side, having the lowest hardness (Fig. 8b). Although these results were close to one another, the FSWed joints yielded higher tensile test results.

3.5. Bending test results

Bending tests were conducted on the upper and lower surfaces of the joints (upper surface and root bending) to see how the samples welded by GMAW and FSW responded to bending stress. This was done to see how ductile the surface of the face-welded joints (or its nearby zones) was, as well as whether there was any defect on the joint or nearby surface. Figure 9 shows the bending behaviour images of the samples welded by GMAW and FSW. The results of bending tests showed that both primary materials could successfully bend by 180°. Top and bottom surface images of the samples welded using GMAW and FSW indicated that no fracture or cracking occurred in any of the welding parameters in the 180° bending test. There were no discontinuity errors (e.g., lack of melting, cracks) in the bending zone of the welded samples. The heat emerging during welding resulted in a softened weld zone and the decreasing of hardness properties gained from the base metals during production [24]. This, in turn, caused the weld zone to become more ductile and thus not crack during bending. In industrial production, manufacturers desire and expect to shape and use welded joints of dissimilar materials according to post-welding construction. Such construction materials thus must successfully pass these tests so that no damage (e.g., cracking or fracture) occurs when exposed to deformation. Therefore, sam-

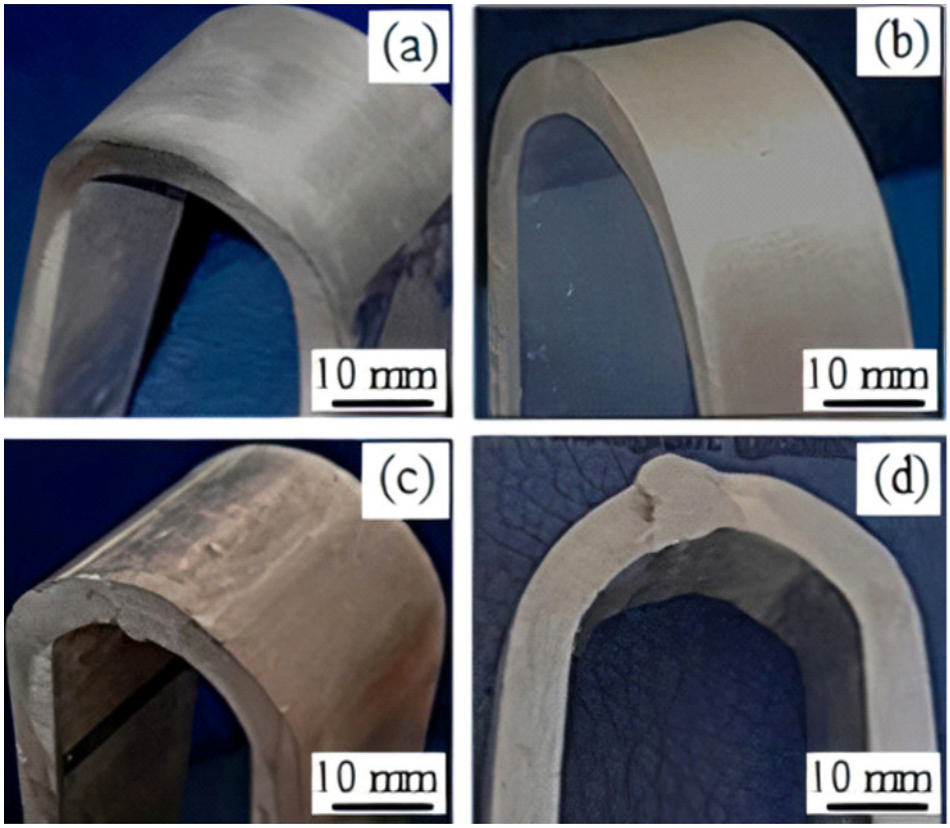

Fig. 9. Images of the samples after the bending test: (a) upper surface of FSW, (b) root of FSW, (c) upper surface of MIG, and (d) root of MIG.

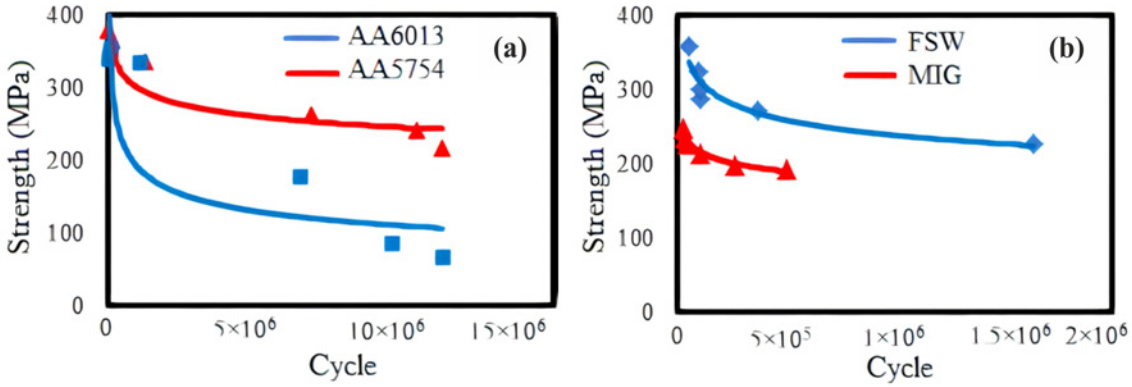

Fig. 10. Fatigue test results: (a) base metals and (b) welded samples.

ples welded using GMAW and FSW can be used safely when bent up to 180° according to post-welding service conditions.

3.6. Fatigue test results

Figure 10 shows fatigue test results of AA5754 and AA6013 aluminium alloys, as well as the GMAW- and FSW-welded AA5754/AA6013 aluminium alloy samples. The fatigue results of the base metals revealed that 10^7 cycles were reached in both base metals without any rupture or fracture. In this case, the experiments demonstrated that AA5754 and AA6013 aluminium alloys had infinite fatigue life. A comparison of the fatigue tests results of the AA6013 and AA5754 base materials revealed that the fatigue life and strength of AA5754 aluminium alloy were lower than those of AA6013 aluminium alloy. T6 ageing heat treatment applied during the production of AA6013 aluminium alloy caused this alloy to gain high

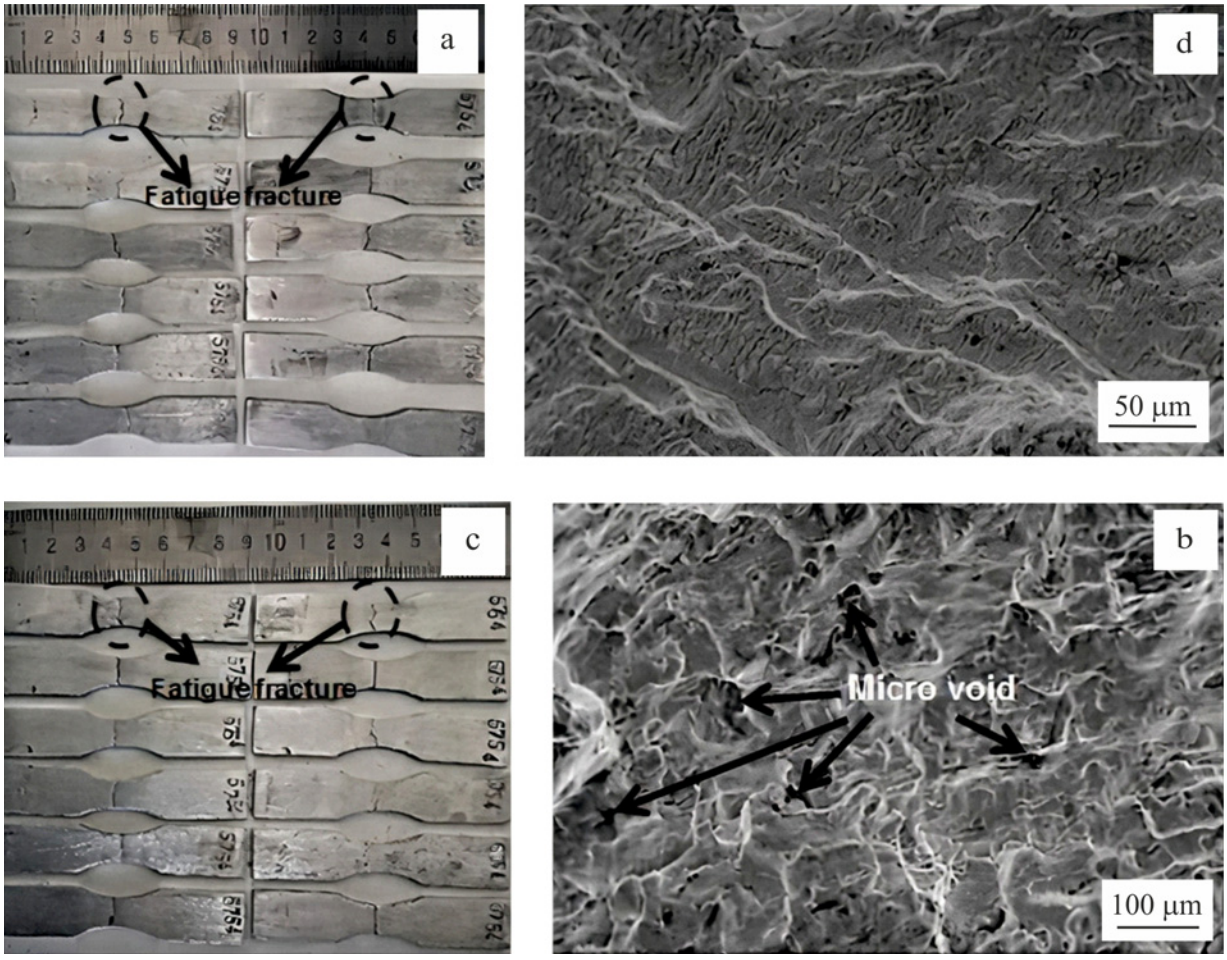

Fig. 11. Weld fracture behaviour and SEM image surfaces of fatigue test samples: (a) and (b) FSWed samples, (c) and (d) samples of GMAW.

strength and high hardness. Likewise, the fatigue lives of welded samples were lower compared to those of the base metals. One reason behind this is heat input during the GMAW and FSW, and thus the post-welding cooling rate reduced the mechanical properties that the materials acquired. Also, the joining processes covered two different aluminium materials, and the mechanical/metallurgical/microstructural properties of weld metal obtained with additional metal were different from both base metals. Similarly, structural defects took place during and after welding [32]. Hence, the fatigue life of the weld metal in the welded joints was lower than the fatigue strength of the base materials – this is normal. A closer look at the fatigue lives of the samples welded by GMAW and FSW revealed that FSWed joints performed better than their GMAW counterparts. This is because the heat input exposed by the weld zone was lower in FSW than GMAW. Low heat input during FSW caused less loss in the metallurgical transformation of base metals in the weld zone as well as mechanical properties they gained during production. This caused the FSWed joint to have a higher fatigue life.

Figure 11 shows fracture surface macro and SEM images of the samples, joined by GMAW and FSW methods, after the fatigue test. Fatigue cracks occurred in the welded samples in the zones that contained the weld seams. These fractures were mainly observed in the zone where the cross-section dimensions of the fatigue sample were the lowest (weld seam). The fracture surface images revealed very few micro-voids, as in the samples welded using both GMAW and FSW. Moreover, fatigue cracks occurred on the fracture surface of the sample welded using GMAW. Micro-void defects may occur in the weld seam, even if it is small, due to rapid solidification during welding – and even if all welding parameters were selected for their optimum values during the fusion welding processes. Zhongjie et al. [34] applied a fatigue test of Al-Zn aluminium alloy they joined by FSW and MIG welding methods and found that the samples occurred at the HAZ interface and the weld metal due to micropores and impurities. Therefore, micro-void defects occurred locally in the weld metals of some of the samples welded using GMAW. The same defects were also found in the FSWed sam-

ple. These microvoids were thought to initiate fatigue cracks during fatigue tests. When conducting fatigue tests, micro-voids cause stress density to increase – thus resulting in the formation and progression of fatigue cracks. Lei et al. [35] reported that joint defects and micro-defects in the weld led to fatigue cracks.

4. Conclusions

In this study, the researchers welded AA5754 and AA6013 using automatic GMAW and FSW and analysed the macrostructural, microstructural, and mechanical properties of welded joints. Their results are summarised below:

1. AA5754/AA6013 aluminium alloy plates were successfully welded using automatic GMAW and FSW.

2. The weld zone of the aluminium alloys welded using both methods showed significant differences. In the samples welded by GMAW, the grains in both weld metal (dendritic grains) and the HAZ became coarse. The intense deformation that occurred during FSW caused the weld metal to be made up of coaxial grains. In addition, micro-void defects occurred in the transition zones of the weld seams.

3. The AA6013 aluminium alloy side in all of the samples welded using both methods had the highest hardness values. The hardness value increased from the welding centre towards AA6013 aluminium alloy and decreased towards AA5754.

4. The tensile strength of the welded joints was lower than the tensile strength of both base metals. The tensile strength of the FSWed sample was higher than that of the sample welded by GMAW.

5. All samples welded using both methods were successfully bent from the upper and lower surfaces at an angle of 180°, without any crack or fracture.

6. The fatigue test results revealed that both fatigue strengths and lives of the base materials were higher than those of the welded samples. The life span of the FSWed sample was higher than that of the GMAW-welded one.

Acknowledgement

The authors would like to thank the Karabük University Scientific Research Project Committee for funding KBUBAP-17-DR-406.

References

[1] R. E. Sanders Jr., P. Hollinshead, E. A. Simielli, Industrial development of non-heat treatable aluminum alloys, Materials Forum 28 (2004) 53–64.

[2] J. Hirsch, Aluminium in innovative lightweight car design, Materials Transactions 52 (2011) 818–824. doi:10.2320/matertrans.L-MZ201132

[3] B. E. Tawfik, H. Leheta, A. Elhewy, T. Elsayed, Weight reduction and strengthening of marine hatch covers by using composite materials, International Journal of Naval Architecture and Ocean Engineering 9 (2017) 185–198. doi:10.1016/j.ijnaoe.2016.09.005

[4] H. Helms, U. Lambrecht, The potential contribution of light-weighting to reduce transport energy consumption, The International Journal of Life Cycle Assessment 12 (2007) 58–64. doi:10.1065/lca2006.07.258

[5] J. Liu, M. J. Tan, A. E. W. Jarfors, Y. Aue-u-lan, S. Castagne, Formability in AA5083 and AA6061 alloys for light weight applications, Materials and Design 31 (2010) 66–70. doi:10.1016/j.matdes.2009.10.052

[6] H. C. Kim, T. J. Wallington, Life-cycle energy and greenhouse gas emission benefits of lightweighting in automobiles: review and harmonisation, Environmental Science & Technology 47 (2013) 6089–6097. doi:10.1021/es3042115

[7] B. Çevik, B. Gülenç, The effect of welding speed on mechanical and microstructural properties of 5754 Al (AlMg3) alloy joined by laser welding, Materials Research Express 5 (2018) 086520. doi:10.1088/2053-1591/aad3b0

[8] A. Heinz, A. Haszler, C. Keidel, S. Moldenhauer, R. Benedictus, W. S. Miller, Recent development in aluminium alloys for aerospace applications, Materials Science and Engineering A 280 (2000) 102–107. doi:10.1016/S0921-5093(99)00674-7

[9] B. Ertuğ, L. C. Kumruoğlu, 5083 type Al-Mg and 6082 type Al-Mg-Si alloys for ship building, American Journal of Engineering Research 4 (2015) 146–150.

[10] G. İpekoğlu, S. Erim, B. G. Kiral, G. Çam, Investigation into the effect of temper condition on friction stir weldability of AA6061 Al-alloy plates, Kovove Mater. 51 (2013) 155–163. doi:10.4149/km-2013-3-155

[11] P. H. Shah, V. J. Badheka, Friction stir welding of aluminium alloys: An overview of experimental findings – Process, variables, development and applications, Journal of Materials: Design and Applications 233 (2019) 1191–1226. doi:10.1177/1464420716689588

[12] J. Rapp, C. Glumann, F. Dausinger, H. Hugel, Laser welding of aluminium lightweight materials: problems, solutions, readiness for application, Optical and Quantum Electronics 27 (1995) 1203–1211. doi:10.1007/BF00326476

[13] N. Murali, M. Sokoluk, G. Yao, S. Pan, I. De Rosa, X. Li, Gas-tungsten arc welding of dissimilar aluminum alloys with nano-treated filler, Journal of Manufacturing Science and Engineering 143 (2021) 081001. doi:10.1115/1.4049849

[14] G. Cornacchia, S. Cecchel, Study and characterisation of EN AW 6181/6082-T6 and EN AC 42100-T6 aluminum alloy welding of structural applications: metal inert gas (MIG), cold metal transfer (CMT), and fiber laser-MIG hybrid comparison, Metals 10 (2020) 441. doi:10.3390/met10040441

[15] S. Yan, Q. H. Qin, H. Chen, Z. Zhong, Hybrid laser welding of dissimilar aluminum alloys: welding processing, microstructure, properties and modelling, Journal of Manufacturing Processes 56 (2020) 295–305. doi:10.1016/j.jmapro.2020.03.048

[16] G. Çam, G. İpekoğlu, Recent developments in joining of aluminum alloys, The International Journal of Advanced Manufacturing Technology 91 (2017) 1851–1866. doi:10.1007/s00170-016-9861-0
[17] S. Vijay, S. Rajanarayanan, G. N. Ganeshan, Analysis on mechanical properties of gas tungsten arc welded dissimilar aluminium alloy (Al2024 & Al6063), Materials Today: Proceedings 21 (2020) 384–391. doi:10.1016/j.matpr.2019.06.136
[18] B. Çevik, Y. Özçatalbaş, B. Gülenç, Friction stir welding of 7075-T651 aluminium alloy, Practical Metallography 53 (2016) 6–23. doi:10.3139/147.110363
[19] G. Çam, S. Mistikoglu, Recent developments in friction stir welding of Al-alloys, Journal of Materials Engineering and Performance 23 (2014) 1936–1953. doi:10.1007/s11665-014-0968-x
[20] B. Çevik, Y. Özçatalbaş, B. Gülenç, Effect of welding speed on the mechanical properties and weld defects of 7075 Al alloy joined by FSW, Kovove Mater. 54 (2016) 241–247. doi:10.4149/km_2016_3_241
[21] A. Özer, A. Şik, B. Çevik, M. Özer, The effect of friction stir welding parameters on microstructure and fatigue strength of CuZn37 brass alloys, Kovove Mater. 55 (2017) 107–114. doi:10.4149/km_2017_2107
[22] E. Taban, E. Kaluc, Microstructural and mechanical properties of double-sided MIG, TIG and friction stir welded 5083-H321 aluminum alloy, Kovove Mater. 44 (2006) 25–33.
[23] B. Çevik, Gas tungsten arc welding of 7075 aluminum alloy: microstructure properties, impact strength, and weld defects, Materials Research Express 5 (2018) 066540. doi:10.1088/2053-1591/aacbbc
[24] B. Çevik, M. Koç, The effects of welding speed on the microstructure and mechanical properties of marine-grade aluminium (AA5754) alloy joined using MIG welding, Kovove Mater. 57 (2019) 307–316. doi:10.4149/km_2019_5_307
[25] H. Ates, A. T. Özdemir, M. Uzun, I. Uygur, Effect of deep sub-zero treatment on mechanical properties of AA5XXX aluminum plates adjoined by MIG welding technique, Scientia Iranica 24 (2017) 1950–1957. doi:10.24200/SCI.2017.4285
[26] E. Mercan, Y. Ayan, N. Kahraman, Investigation on joint properties of AA5754 and AA6013 dissimilar aluminum alloys welded using automatic GMAW, Engineering Science and Technology, an International Journal 23 (2020) 723–731. doi:10.1016/j.jestch.2019.11.004
[27] P. P. Lean, L. Gil, A. Ureña, Dissimilar welds between unreinforced AA6082 and AA6092/SiC/25p composite by pulsed-MIG arc welding using unreinforced filler alloys (Al-5Mg and Al-5Si), Journal of Materials Processing Technology 143 (2003) 846–850. doi:10.1016/S0924-0136(03)00331-5
[28] C. Caglioni, F. M. Rigon, M. A. Losekann, L. C. S. H. Rezende, M. V. P. Companhoni, M. Corso, S. L. Favaro, Similar and dissimilar welding effect on the mechanical properties of 5383 H34, 5754 H34 and 6005 T6 aluminum alloys, Matéria (Rio de Janeiro) 25 (2020). doi:10.1590/s1517-707620200002.1009
[29] E. G. Cole, A. Fehrenbacher, N. A. Duffie, M. R. Zinn, F. E. Pfefferkorn, N. J. Ferrier, Weld temperature effects during friction stir welding of dissimilar aluminum alloys 6061-T6 and 7075-T6, The International Journal of Advanced Manufacturing Technology 71 (2014) 643–652. doi:10.1007/s00170-013-5485-9
[30] N. Khanna, P. Sharma, M. Bharati, V. J. Badheka, Friction stir welding of dissimilar aluminium alloys AA 6061-T6 and AA 8011-H14: a novel study, Journal of the Brazilian Society of Mechanical Sciences and Engineering 42 (2020) 7. doi:10.1007/s40430-019-2090-3
[31] I. Uygur, Influence of shoulder diameter on mechanical response and microstructure of FSW welded 1050 Al-alloy, Archives of Metallurgy and Materials 57 (2012) 53–60. doi:10.2478/v10172-011-0152-3
[32] Ç. Yeni, S. Sayer, M. Pakdil, Comparison of mechanical and microstructural behaviour of TIG, MIG and friction stir welded 7075 aluminium alloy, Kovove Mater. 47 (2009) 341–347.
[33] T. Azimzadegan, S. Serajzadeh, An investigation into microstructures and mechanical properties of AA7075-T6 during friction stir welding at relatively high rotational speeds, Journal of Materials Engineering and Performance 19 (2010) 1256–1263. doi:10.1007/s11665-010-9625-1
[34] Y. Zhongjie, L. Xuesong, F. Hongyuan, Mechanical properties of friction stir welding and metal inert gas welding of Al-Zn aluminum alloy joints, The International Journal of Advanced Manufacturing Technology 91 (2017) 3025–3031. doi:10.1007/s00170-017-0021-y
[35] W. Lei, H. Li, Z. Song, X. Liang, H. Bo, Effect of corrosive environment on fatigue property and crack propagation behavior of Al 2024 friction stir weld, Transactions of Nonferrous Metals Society of China, 26 (2016) 2830–2837. doi:10.1016/S1003-6326(16)64411-4